

**UNCLASSIFIED**

---

**AD 273 837**

*Reproduced  
by the*

**ARMED SERVICES TECHNICAL INFORMATION AGENCY  
ARLINGTON HALL STATION  
ARLINGTON 12, VIRGINIA**



---

**UNCLASSIFIED**

NOTICE: When government or other drawings, specifications or other data are used for any purpose other than in connection with a definitely related government procurement operation, the U. S. Government thereby incurs no responsibility, nor any obligation whatsoever; and the fact that the Government may have formulated, furnished, or in any way supplied the said drawings, specifications, or other data is not to be regarded by implication or otherwise as in any manner licensing the holder or any other person or corporation, or conveying any rights or permission to manufacture, use or sell any patented invention that may in any way be related thereto.

597

273837

CATALOGED BY ASTIA  
AS AD NO.

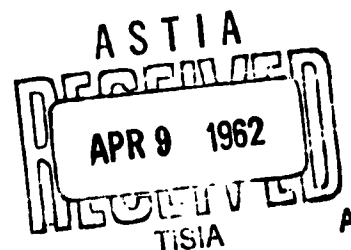
HEAT TRANSFER AND TEMPERATURE  
DISTRIBUTION IN A HEMISPHERICAL  
NOSE CONE IN HYPERSONIC FLOW

by

S. V. Nardo and Ronald W. Sadler



110 200



POLYTECHNIC INSTITUTE OF BROOKLYN

DEPARTMENT  
of  
AEROSPACE ENGINEERING  
and  
APPLIED MECHANICS

JANUARY 1962

PIBAL REPORT NO. 597

Contract No. Nonr 839(23)  
Project No. NR 064-433

HEAT TRANSFER AND TEMPERATURE DISTRIBUTION  
IN A HEMISPHERICAL NOSE CONE  
IN HYPERSONIC FLOW

by

S. V. Nardo and Ronald W. Sadler

Polytechnic Institute of Brooklyn  
Department of  
Aerospace Engineering and Applied Mechanics

January 1962

PIBAL Report No. 597

Reproduction in whole or in part is permitted for any purpose of  
the United States Government.

## TABLE OF CONTENTS

	Page
1. ABSTRACT. . . . .	1
2. LIST OF SYMBOLS . . . . .	2
3. INTRODUCTION. . . . .	4
4. THEORETICAL HEAT TRANSFER CALCULATIONS. . . . .	6
5. COMPARISON WITH EXPERIMENTS . . . . .	11
6. TEMPERATURE DISTRIBUTION. . . . .	15
7. CONCLUSIONS . . . . .	17
8. ACKNOWLEDGEMENT . . . . .	18
9. REFERENCES. . . . .	19
10. TABLES. . . . .	21
11. FIGURES . . . . .	22

## 1. ABSTRACT

The heat transfer to a hemispherical nose cone subjected to hypersonic flow conditions is calculated for three Reynolds Numbers. The theory is compared with the results of test runs at these Reynolds Numbers on a stainless steel hemisphere in the Polytechnic hypersonic tunnel facility. Except for the region of highest (theoretical) heat input, the comparison is good.

Using the theoretical heat transfer results in conjunction with the one-dimensional transient heat conduction solution through a spherical shell element, temperature histories are obtained at selected points in the interior of the hemispherical nose cone. A comparison with experimental data shows a satisfactory agreement.

It is concluded that the theoretical heat transfer values used in conjunction with the one-dimensional transient heat conduction solution through a spherical shell element, are adequate for predicting the temperature distribution within the hemispherical nose cone. The restrictions are to flows with a Reynolds Number range of from one to five million, stagnation temperatures less than  $4000^{\circ}\text{R}$ , and pressure distributions similar to that given in this report.

## 2. SYMBOLS

(B)	buried thermocouple, located midway between heated and insulated (inner) surfaces
$C_f$	local skin friction coefficient
$f''$	Blasius non-dimensional friction factor
$h$	enthalpy
(H)	thermocouple located on heated surface
(I)	thermocouple located on insulated surface
$k$	thermal conductivity
$N_R$	Reynolds number, $\rho_{s_e} (h_{s_e})^{1/2} R_o / \mu_{s_e}$
$\tilde{N}_R$	$N_R \phi_{s_e}^{1/2}$
$N_{R_\theta}$	Reynolds number based on momentum thickness, $\rho_e u_e \theta / \mu_e$
$N_u$	Nusselt number, $q_w R_o / (T_{s_e} - T_w) k_{s_e}$
$P$	pressure
$P_r$	Prandtl number
$q$	heat transfer per unit area per unit time
$r$	perpendicular distance from surface to centerline of hemisphere
$\bar{r}$	$r/R_o$
$R_o$	external nose radius of hemisphere
$s$	distance along surface measured from the stagnation point along a meridian
$\bar{s}$	$s/R_o$
$T$	temperature
$\bar{T}$	$(T_s - T)/(T_s - T_i)$

$u$	local velocity at edge of boundary layer
$\bar{u}$	$u/(h_{s_e})^{1/2}$
$\beta$	pressure gradient parameter
$\delta^*$	boundary layer displacement thickness
$\varphi_{s_e}$	$p_s/\rho_{s_e} h_{s_e}$
$\theta$	momentum thickness
$\mu$	viscosity coefficient
$\bar{\mu}$	$\mu_e/\mu_{s_e}$
$\rho$	mass density
$\bar{\rho}$	$\rho_e/\rho_{s_e}$
$\tau$	shear stress

#### Subscripts

aw	adiabatic wall
e	conditions external to the boundary layer
i	initial conditions
s	stagnation conditions
w	wall conditions



### 3. INTRODUCTION

This report is one of a series dealing with the general problem of temperatures, deformations, and material changes of a hemispherical configuration in a hypersonic flow environment. The principal purpose of this report is to present a simple method for predicting the temperature distribution within the hemispherical body under certain restricted hypersonic flow conditions. A reasonably accurate knowledge of the temperature distribution will be necessary for subsequent theoretical studies of stresses and deformations, and for the interpretation of experimental results.

First, a theoretical analysis is made of the heat transfer to a hemispherical body under hypersonic conditions for laminar, turbulent, and transition boundary layer regions. The results are compared with experimental heat transfer data obtained on a hemispherical nose cone configuration in the Polytechnic hypersonic facility.

Except for the region of highest heat input, the agreement between theory and experiment is sufficiently satisfactory to suggest the following simplification in the temperature distribution estimation within the hemisphere. The local theoretical heat transfer coefficient is used in conjunction with the transient one-dimensional heat conduction solution for spherical shell elements. Temperature-time histories at selected points in the interior are compared with available test data and the agreement is

found to be quite satisfactory for purposes of future estimation of temperatures on similar models which are not equipped with thermocouple instrumentation.

Future hemispherical nose cone models of various thicknesses, but of similar external configuration will be instrumented only on the inner, or insulated surface. Thus, if the method of estimating temperatures presented in this report is reasonably accurate, these predictions can be used to obtain the physical properties of materials from data available on the variation of these properties with temperature, to calculate thermal stresses, and for any purpose requiring a knowledge of the temperature to make calculations and to evaluate experimental data.

#### 4. THEORETICAL HEAT TRANSFER CALCULATIONS

The heat transfer to a hemispherical configuration under hypersonic conditions was calculated for three values of the Reynolds Number,  $\tilde{N}_R$ :  $0.97 \times 10^6$ ,  $3.3 \times 10^6$  and  $5.1 \times 10^6$ . The Reynolds Numbers were chosen to coincide with the values at which hypersonic tunnel tests had previously been run on a stainless steel hemisphere. This stainless steel model was specifically designed to obtain experimental values of the heat and load input. Complete data are reported in Ref. [1], but a brief description of the model and tests are given in Section 5.

The technique for predicting the laminar heat transfer under the above conditions may readily be obtained from Ref. [2], [3], and [4]. In Ref. [2], Lees provides the most convenient method for estimating the laminar heat transfer under hypersonic conditions. It involves the assumption of a constant value of pressure gradient parameter,  $\beta$ , in the transformed coordinate system; a ratio of wall to stagnation enthalpy, small compared to unity, and a linear dependence of viscosity on temperature ( $\rho_e \mu_e = \rho_w \mu_w$ ). There results a simple numerical evaluation of an integral of external flow properties and radius to determine the heat transfer distribution.

In terms of the variables used here, the theory of Lees gives

$$\frac{N_u}{N_R^{1/2}} = (0.353) P_r^{1/3} (\phi_{s_e})^{-1/4} \cdot \frac{\bar{\rho} \bar{u} \bar{\mu} \bar{r}}{[\int_0^{\bar{s}} \bar{\rho} \bar{u} \bar{\mu} \bar{r}^2 d\bar{s}]^{1/2}}$$

The limiting process for obtaining the stagnation point value from the above equation leads to the axially symmetric stagnation point heat transfer ( $\bar{\rho} \rightarrow 1$ ,  $\bar{u} \rightarrow \bar{\beta} \bar{s}$  etc.). This gives

$$\frac{N_u}{\tilde{N}_R^{1/2}} = (0.706) P_r^{1/3} (\phi_{s_e})^{-1/4} (\bar{\beta})^{1/2}$$

where

$$\bar{\beta} = (d\bar{u}/d\bar{s}) \quad \text{at} \quad \bar{s} = 0.$$

The technique involving the determination of the transitional and turbulent heat transfer requires the determination of the transition point on the model.  $N_{R_\theta}$  values of 200 and 300 were chosen for this model. These transition Reynolds Numbers are based on experimental results performed by various investigators.

Before starting the analysis of the turbulent boundary layer, it is necessary to evaluate the laminar coefficient of wall friction at the transitional point.

By definition, the wall friction coefficient is:

$$C_f/2 = \tau_w / (\rho_e u_e^2) .$$

Through Lees transformation,

$$C_f/2 = \frac{\mu_e R_\theta}{(2s)^{1/2}} f_w'' ,$$

which may be written as

$$C_f/2 = 0.22/N_{R_\theta} .$$

To evaluate the wall friction coefficient in the transitional and fully turbulent flow regimes, the friction law developed in Ref. [5] was adopted.

$$C_f/2 = \bar{\mu} \left[ \frac{0.013}{N_{R_\theta}^{1/4}} - \frac{B}{N_{R_\theta}^n} \right]$$

This law is similar in form to that developed by Persh, Ref. [6]. The value of  $n$  was taken as 1, as suggested in Ref. [9].

The constant  $B$  of this law is evaluated from the laminar flow such that the friction coefficient  $C_f/2$  remains continuous at the laminar to turbulent transition point.

$$B = \left[ N_{R_\theta}^n \left( \frac{0.013}{N_{R_\theta}^{1/4}} - \frac{C_f}{2} \frac{\mu_s}{\mu_e} \right) \right]_{\text{trans.}}$$

In order to obtain the heat transfer, a stepwise solution of the boundary layer momentum equation is obtained through the use of boundary layer form factors which are based on a correlation of incompressible data.

$$\frac{d\theta}{ds} = (C_f/2) - \theta \left[ \frac{(\delta^*/\theta) + 2}{u_e} \frac{du_e}{ds} + \frac{1}{\rho_e} \frac{d\rho_e}{ds} + \frac{1}{r} \frac{dr}{ds} \right]$$

In this work, following the suggestion of Ref. [5], the form factor was taken as:

$$H_e = (\delta^*/\theta) \approx -1.$$

The heat transfer is calculated from

$$q_w = P_r^{-(2/3)} (h_{aw} - h_w) \rho_e u_e (C_f/2)$$

and finally

$$N_u = P_r^{1/3} \left( \frac{h_{aw} - h_w}{h_{se} - h_w} \right) \frac{\overline{\rho u}}{\phi_{se}^{1/2}} (C_f/2) \tilde{N}_R.$$

The theoretical distribution of heat transfer along a meridian for a laminar boundary layer is shown in Fig. 1. The heat transfer parameter  $(N_u/N_R^{1/2})$  correlates the heat transfer for any value of the Reynolds Number. In the transition and turbulent boundary layer range, however, the calculations were made

for three specific values of the Reynolds Number. Fig. 2 presents the results of calculations based on a transition-turbulent boundary layer for Reynolds Numbers of  $0.97 \times 10^6$ ,  $3.3 \times 10^6$  and  $5.1 \times 10^6$ . Transition from laminar boundary layer is assumed to occur at a Reynolds Number based on a momentum thickness ( $N_{R_\theta}$ ) of 250. The heat transfer parameter  $N_u / \tilde{N}_R^{4/5}$  is plotted against distance along the meridian from the stagnation point. In Fig. 3, the same calculations, based on a transition value of  $N_{R_\theta} = 300$  are graphically presented.

## 5. COMPARISON WITH EXPERIMENTS

In Ref. [1], the results of 6 test runs at simulated hypersonic speeds on a hemispherical model were reported in both graphical and tabular form. The model was fabricated of Type 304 stainless steel, had a 7-3/4 inch outside diameter and one-inch wall. It was extensively instrumented with pressure taps and thermocouples. The principal mission of these tests was to obtain basic data on both the aerodynamic and thermal loads. Aerodynamic load data were presented in Ref. [1] and are also shown in Fig. 4. (This pressure distribution was used in calculating the theoretical heat transfer). The procedure for obtaining the thermal input, based on the thermocouple temperature-time histories, is outlined below.

The hemispherical model was instrumented with a total of 40 thermocouples, as shown in Fig. 5. Thirteen of these thermocouples were specially constructed one-dimensional plugs for heat transfer work. This instrument was first described in Ref. [7], and further discussed in Ref. [1]. A sketch of a typical thermocouple plug is shown in Fig. 6. The principal virtue of these plugs is the relative ease with which the heat input could be deduced from the temperature-time history of the thermocouple on the heated surface of the model. The remaining thermocouple installations were "standard", and were disposed on the outer and inner surfaces of the model as well as at interior



points. Sketches of a "standard" heated surface thermocouple and a buried thermocouple installation are shown in Figs. 7 and 8.

The experimental values of the heat transfer were deduced from the one-dimensional plug temperature-time histories, and from similar data from the standard thermocouple installations on the outer (heated) surface of the model. In the case of the one-dimensional plugs, the heat conduction equations for the transient one-dimensional flow of heat through a finite slab were solved for the heat input  $q_w$  on the heated side of the slab as a function of time. The other side of the slab was considered to be insulated. The plug temperature-time history was used as a boundary condition. Except for the first few seconds, the values of  $q_w$  thus calculated, resulted in an essentially constant value of the Nusselt Number. The time average of the almost constant value of the Nusselt Number was used as the experimental value presented in this report.

In obtaining the experimental heat transfer from the standard heated surface thermocouples, use was made of the transient heat conduction solution for the flow of heat through a spherical shell element, one-dimensional, outside surface heated, inside surface insulated, Ref. [8]. For the geometry parameter corresponding to the tested model, temperature-time plots were carefully drawn for constant values of the heat transfer coefficient. When the experimental temperature-time history was superimposed upon this set of curves, the heat transfer coefficient

could easily be interpolated at several points and the results averaged. Again, these heat transfer coefficient values were essentially constant after the first few seconds of the test run.

A comparison of the experimental values of the heat transfer thus deduced with the theoretical values is shown in Figs. 9, 10 and 11.

In Fig. 9, for example, the theoretical curves are given in the form of Nusselt Number versus distance along the meridian from the stagnation point for a value of  $\tilde{N}_R = 0.97 \times 10^6$ . These curves are easily obtained from the basic data presented in Figs. 1, 2 and 3. Note, from Table 1, that a value of  $\tilde{N}_R = 0.97 \times 10^6$  corresponds closely to test runs 1 and 2, and hence experimental data from these runs are shown. The experimental data deduced from the one-dimensional plugs are consistently higher than those data deduced from the standard surface thermocouple installations. Near the stagnation point, there is a discrepancy of up to 25% between theory and experiment, but there is an improvement with higher values of  $\bar{s}$ . Unfortunately, it is not altogether certain whether transition occurs at the lowest Reynolds Number,  $0.97 \times 10^6$  (Fig. 9); but if transition does occur it would be at a value of  $\bar{s} > 0.9$ .

Fig. 10 shows the comparison between theory and experiment for  $\tilde{N}_R = 3.3 \times 10^6$ , corresponding to conditions of test runs 3 and 4. A similar presentation for  $\tilde{N}_R = 5.1 \times 10^6$ , corresponding to test run 5 is shown in Fig. 11. Once again it can be noted that experimental heat transfer values from the thermocouple plugs are usually higher than the heat transfer values deduced from the standard surface thermocouple data. In Figs. 10 and 11 there is

no question of transition of the boundary layer from laminar to turbulent. Additional data in the region of highest heat transfer would have been desirable. Several of the instruments in this area, however, were damaged during the installation of the model into the wind tunnel and during the course of the test runs.

On the basis of the comparisons of Figs. 9, 10 and 11, it was decided to take the heat transfer results calculated for the laminar case and for  $N_{R_\theta} = 300$  and use the heat conduction equations through a spherical element to predict the temperatures within the hemispherical model.

## 6. TEMPERATURE DISTRIBUTION

The temperature distribution within the hemispherical model was calculated by utilizing the heat conduction solutions for the transient one-dimensional flow of heat in a spherical shell element, Ref. [8]. For a given  $\bar{s}$  and  $\tilde{N}_R$ , the heat transfer coefficient was taken from Figs. 9, 10, or 11. The inner surface was assumed to be insulated. Temperature-time histories could therefore be obtained at any point within the model, for any of the three Reynolds Number ranges for which the theoretical heat transfer calculations were made.

In the six test runs of Ref. [1], thermocouples were buried at various points within the body (see Fig. 5) and on the inner surface. Therefore, the points selected for computing the temperature-time histories by the above method, included points at which thermocouples were physically located on the model. The obvious purpose was to obtain a comparison between the experimental and the calculated temperature-time histories.

The results of this comparison are presented in Figs. 12 and 13, corresponding to the lowest and highest Reynolds Number, respectively. An examination of these temperature-time histories reveals that the calculated temperatures are usually higher than those measured during the test. ( $\bar{T}$  is defined in such a manner that it will decrease with increasing temperature.) Maximum deviation from the experimentally determined temperatures occurs at

$\bar{s} = 1.4$ ; 6.3% difference at  $\tilde{N}_R = 0.97 \times 10^6$ , and 13.4% difference at  $\tilde{N}_R = 5.1 \times 10^6$ . At the points of highest heat transfer, the percentage error was somewhat less. For example, for runs 1 and 2,  $\tilde{N}_R = 0.97 \times 10^6$ , thermocouples 24 and 36 at  $\bar{s} = 0.698$  gave temperature-time histories for which the maximum deviation from the calculated temperature-time history was approximately 2.5%. At the highest Reynolds Number, the comparable error at the same location was 10%. It may be noted that while the maximum percentage error occurs at the region of highest theoretical heat input, the maximum percentage errors in temperature occurred elsewhere.

The agreement between the experimental and calculated temperature-time histories is good when one considers that the calculated temperatures are based on a one-dimensional heat conduction solution. The fact that the calculated values of the temperature are almost always higher than the experimental values is not wholly unexpected inasmuch as the calculated heat transfer results are generally higher than those deduced from the plugs and surface thermocouples.

## 7. CONCLUSIONS

On the basis of the comparison between theory and experiment of heat transfer and temperature distribution presented in this report, it is concluded that the simplified method used to predict temperatures within a hemispherical nose cone in a hypersonic flow is satisfactory. The restriction must be made to flows in the Reynolds Number range of from  $1 \times 10^6$  to  $5 \times 10^6$ , and to stagnation temperatures less than  $4000^\circ\text{R}$ . In order to apply the method it is first necessary to calculate the theoretical heat transfer for the appropriate Reynolds Number. Using the local values of the heat transfer, in conjunction with the transient, one-dimensional heat conduction solution through a spherical shell element, yields the temperature-time history at any point within the body.

## 8. ACKNOWLEDGEMENT

The authors gratefully acknowledge the assistance of Professors Libby, Cresci, Zakkay and Mr. Economos, of the Aerodynamics Laboratory staff, for their assistance in obtaining the theoretical heat transfer values presented in this report.

Many thanks are also due Messrs. Brown and Parisse for their assistance with the calculations and preparation of the illustrations.

## REFERENCES

1. Nardo, S.V., Boccio, J.L., Erickson, B. and Kempner, J.: Experimental Temperature Distribution in a Hemispherical Nose Cone in Hypersonic Flow, PIBAL Report No. 494, June 1959.
2. Lees, L.: Laminar Heat Transfer Over Blunt-Nosed Bodies at Hypersonic Flight Speeds, Jet Propulsion, Vol. 26, pp. 259-269, April 1956.
3. Fay, J.A., Riddell, F.R. and Kemp, N.J.: Stagnation Point Heat Transfer in Dissociated Air Flow, Jet Propulsion, Vol. 27, No. 6 pp. 672-674, June 1957.
4. Cohen, Clarence B. and Reshotko, Eli: Similar Solutions for the Compressible Laminar Boundary Layer with Heat Transfer and Pressure Gradient, NACA Report 1293, 1956.
5. Cresci, R.J., MacKenzie, D.A. and Libby, P.A.: An Investigation of Laminar, Transitional and Turbulent Heat Transfer on Blunt-Nosed Bodies in Hypersonic Flow, Journal of the Aerospace Sciences, Vol. 27, No. 6, pp. 401-414, June 1960.
6. Persh, J.: A Procedure for Calculating the Boundary Layer Development in the Region of Transition from Laminar to Turbulent Flow, U.S.N.O.L. NAVORD Report 4438, March 1957.
7. Ferri, A. and Libby, P.A.: A New Technique for Investigating Heat Transfer and Surface Phenomena Under Hypersonic Flow Conditions, Journal of the Aerospace Sciences, Vol. 24, No. 6, pp. 464-465, June 1957.



8. Smithson, R.E. and Thome, C.J.: U. S. Naval Ordnance Test Station NAVORD Report 5562, Part 6, NOTS 2088, September 1958.
9. Economos, C. and Libby, P.A.: A Note on Transitional Heat Transfer Under Hypersonic Conditions, Reader's Forum, Journal of the Aerospace Sciences, Vol. 29, No. 1, pp. 101-102, January 1962.

TABLE I

## STAGNATION DATA

Run	$T_s$ (°R)	$P_s$ (psia)	$P_s \times 10^3$ $(\frac{lb \ sec^2}{ft^4})$	$h_s \times 10^{-6}$ $(\frac{ft^2}{sec^2})$	$\mu_s \times 10^6$ $(\frac{lb \ sec}{ft^2})$	$N_R \times 10^{-6}$	$\tilde{N}_R \times 10^{-6}$	$\frac{\mu_{s,D}}{k_s}$	$k_s \times 10^3$ $(\frac{Btu \ in}{ft^2 \ sec^{\circ}F})$
1	1285	21.4	1.398	8.27	.705	1.78	.953	.680	.103
2	1283	22.4	1.463	8.27	.705	1.87	1.00	.689	.102
3	1418	83.8	4.959	9.32	.750	6.23	3.34	.696	.109
4	1462	84.6	4.856	9.65	.763	6.08	3.26	.695	.112
5	1656	152	7.702	11.1	.822	9.51	5.09	.701	.121
6	1865	152	6.839	12.8	.885	8.34	4.47	.713	.132

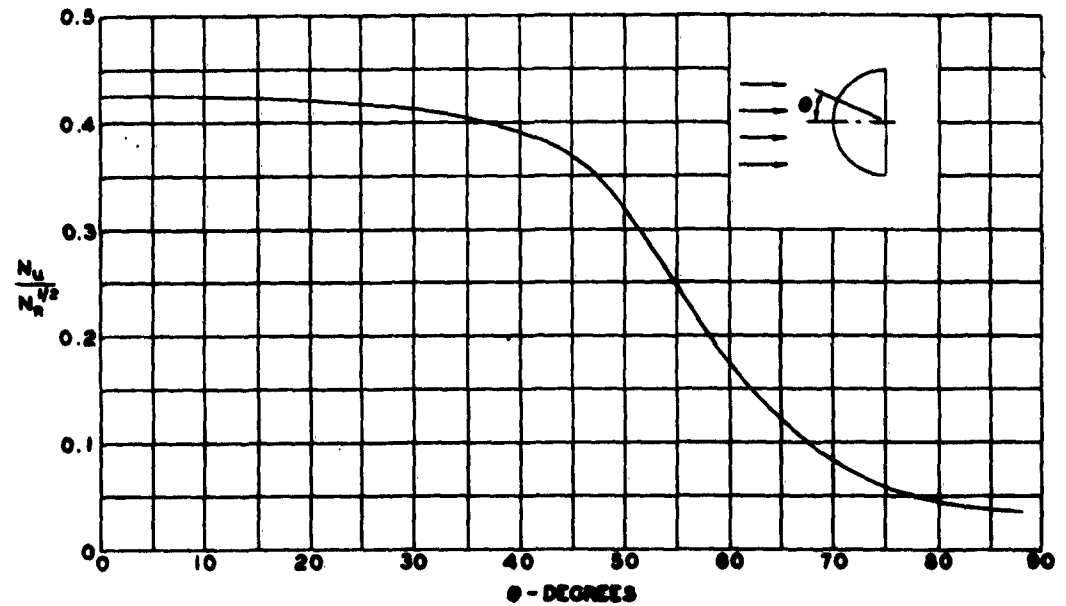


FIG. 1 THEORETICAL DISTRIBUTION OF HEAT TRANSFER ALONG MERIDIAN OF HEMISPHERE LAMINAR BOUNDARY LAYER

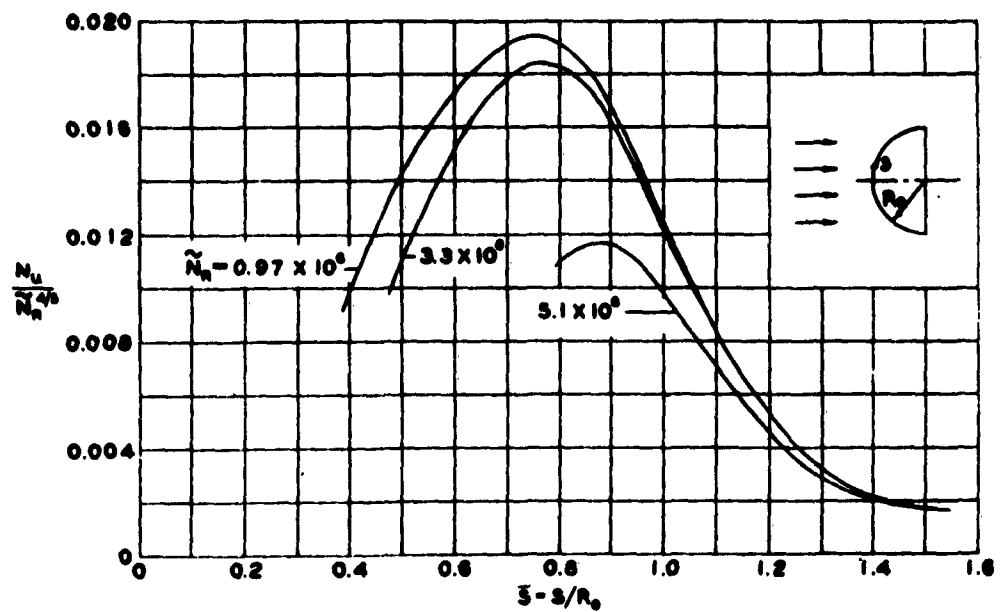


FIG. 2 THEORETICAL DISTRIBUTION OF HEAT TRANSFER ALONG MERIDIAN OF HEMISPHERE TRANSITION - TURBULENT BOUNDARY LAYER  $N_{R_0} = 250$

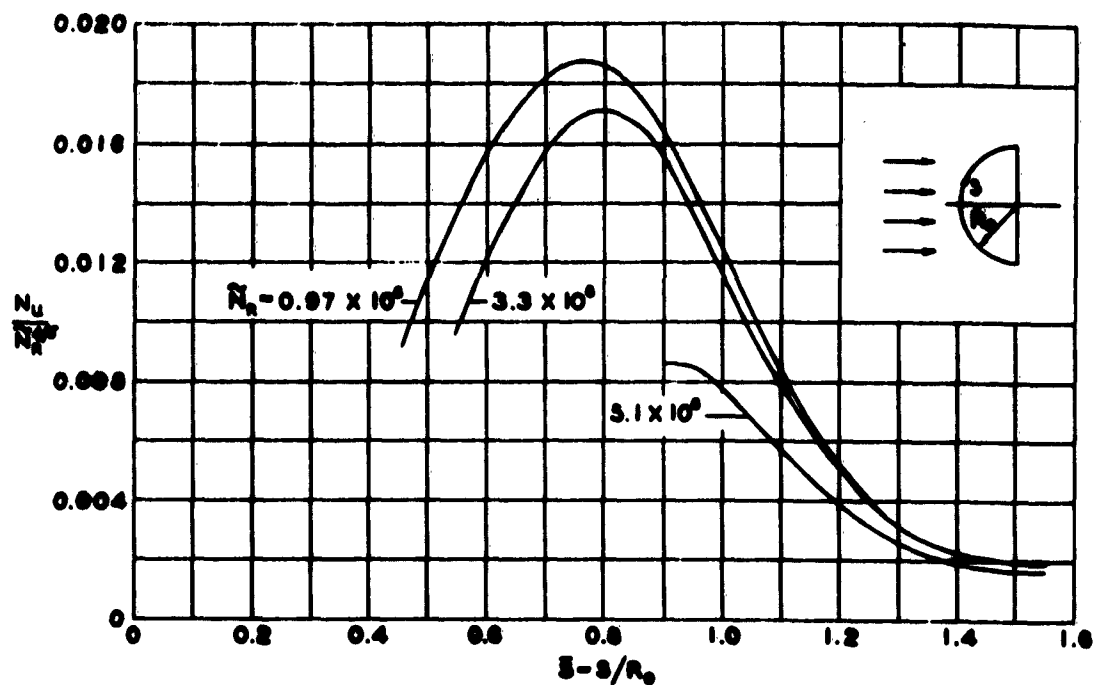


FIG. 3 THEORETICAL DISTRIBUTION OF HEAT TRANSFER ALONG MERIDIAN OF HEMISPHERE  
TRANSITION - TURBULENT BOUNDARY LAYER  
 $Re_0 = 300$

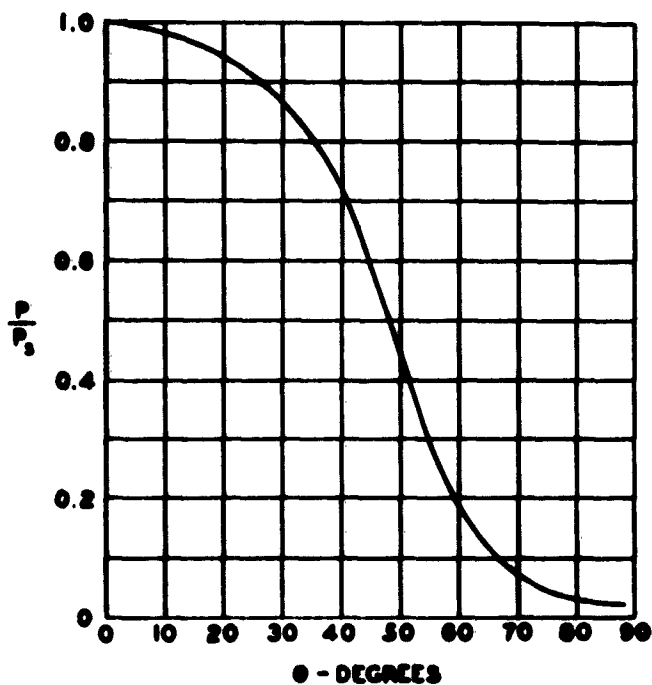
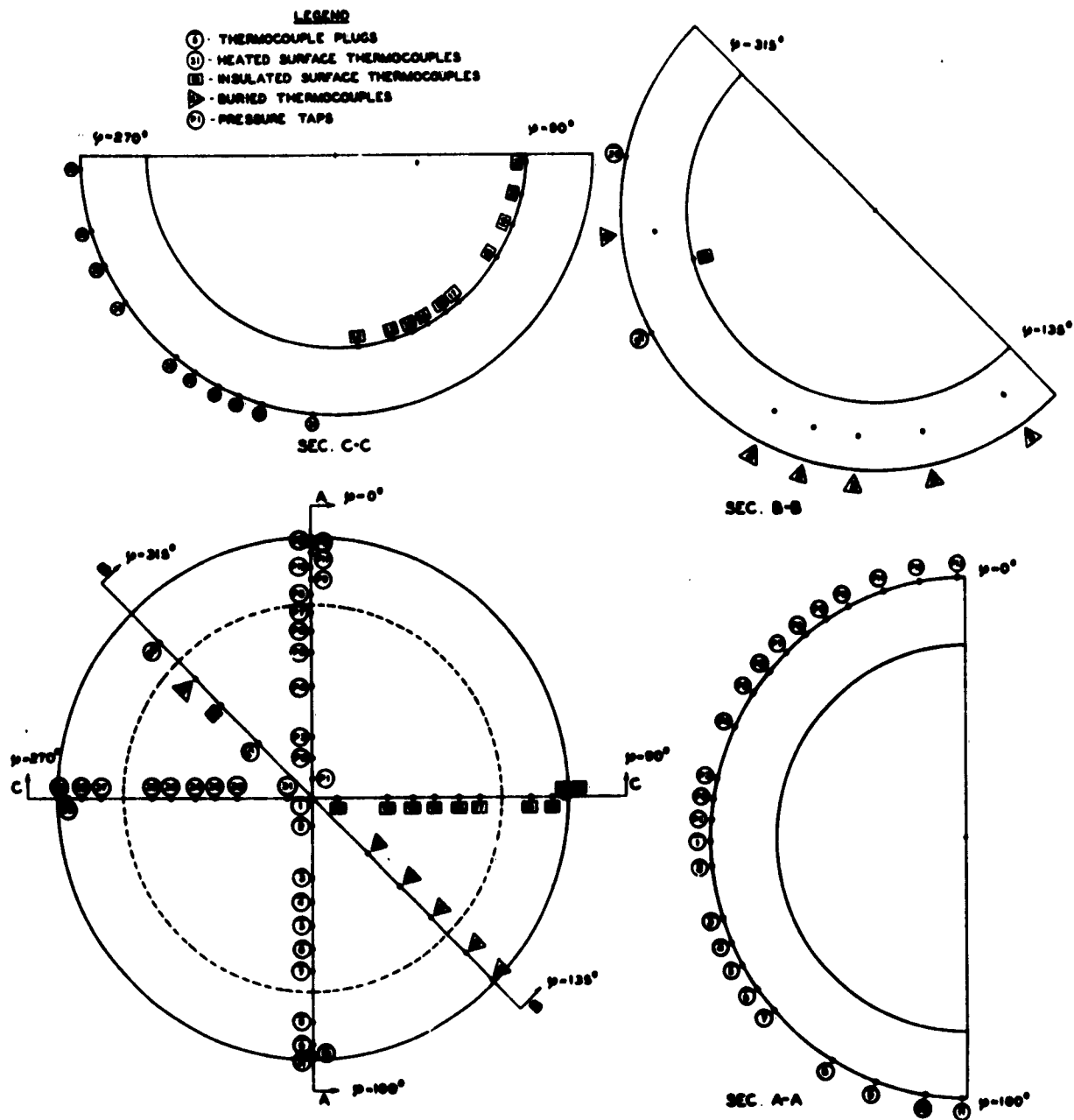


FIG. 4 PRESSURE DISTRIBUTION ON HEMISPHERICAL NOSE CONE  
(FROM TEST DATA OF REF. 1)



**FIG. 5 LOCATION OF INSTRUMENTATION  
MODEL NO. 1  
(REF. 1)**

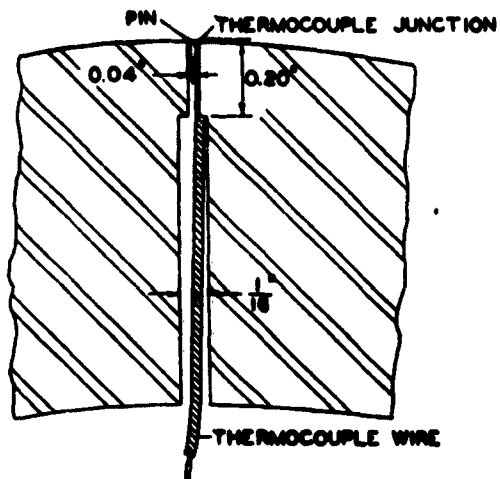


FIG. 7 TYPICAL HEATED SURFACE  
THERMOCOUPLE ASSEMBLY  
(REF. 1)

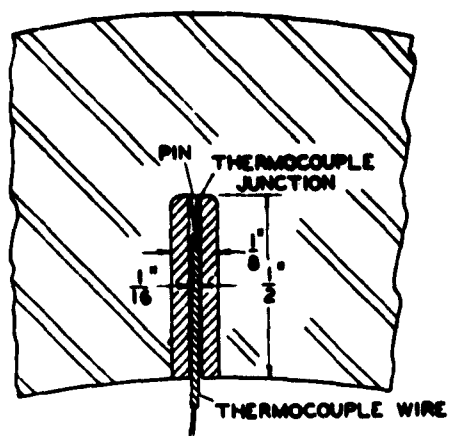


FIG. 8 TYPICAL BURIED  
THERMOCOUPLE ASSEMBLY  
(REF. 1)

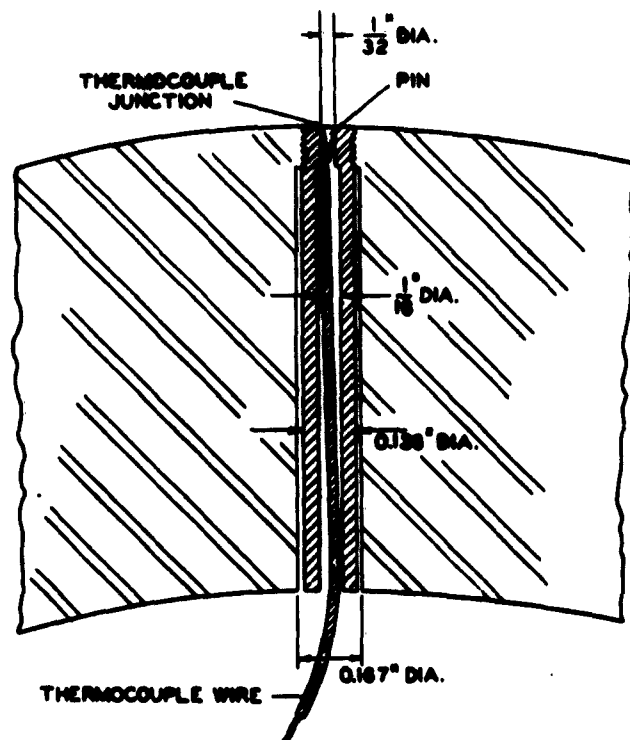


FIG. 6 TYPICAL ONE-DIMENSIONAL  
THERMOCOUPLE PLUG INSTALLATION  
(REF. 1)

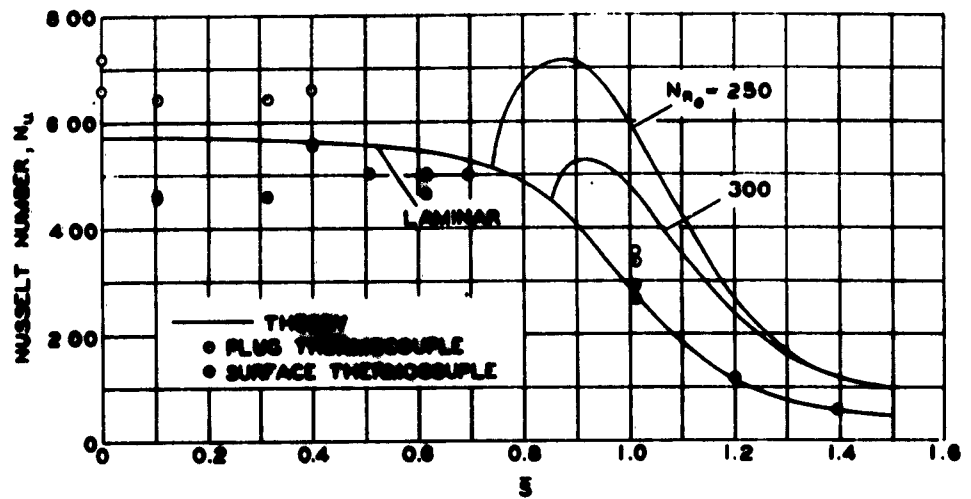


FIG. 9 VARIATION OF NUSSLET NUMBER ALONG MERIDIAN OF HEMISPHERE  
 $\tilde{N}_R = 0.97 \times 10^5$  - RUNS 1 AND 2

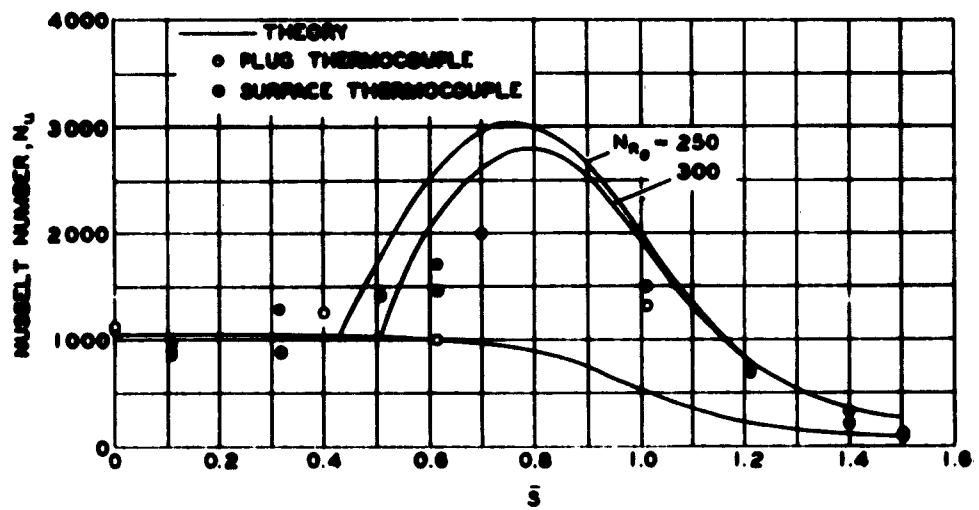


FIG. 10 VARIATION OF NUSSLET NUMBER ALONG MERIDIAN OF HEMISPHERE  
 $\tilde{N}_R = 3.3 \times 10^5$  - RUNS 3 AND 4

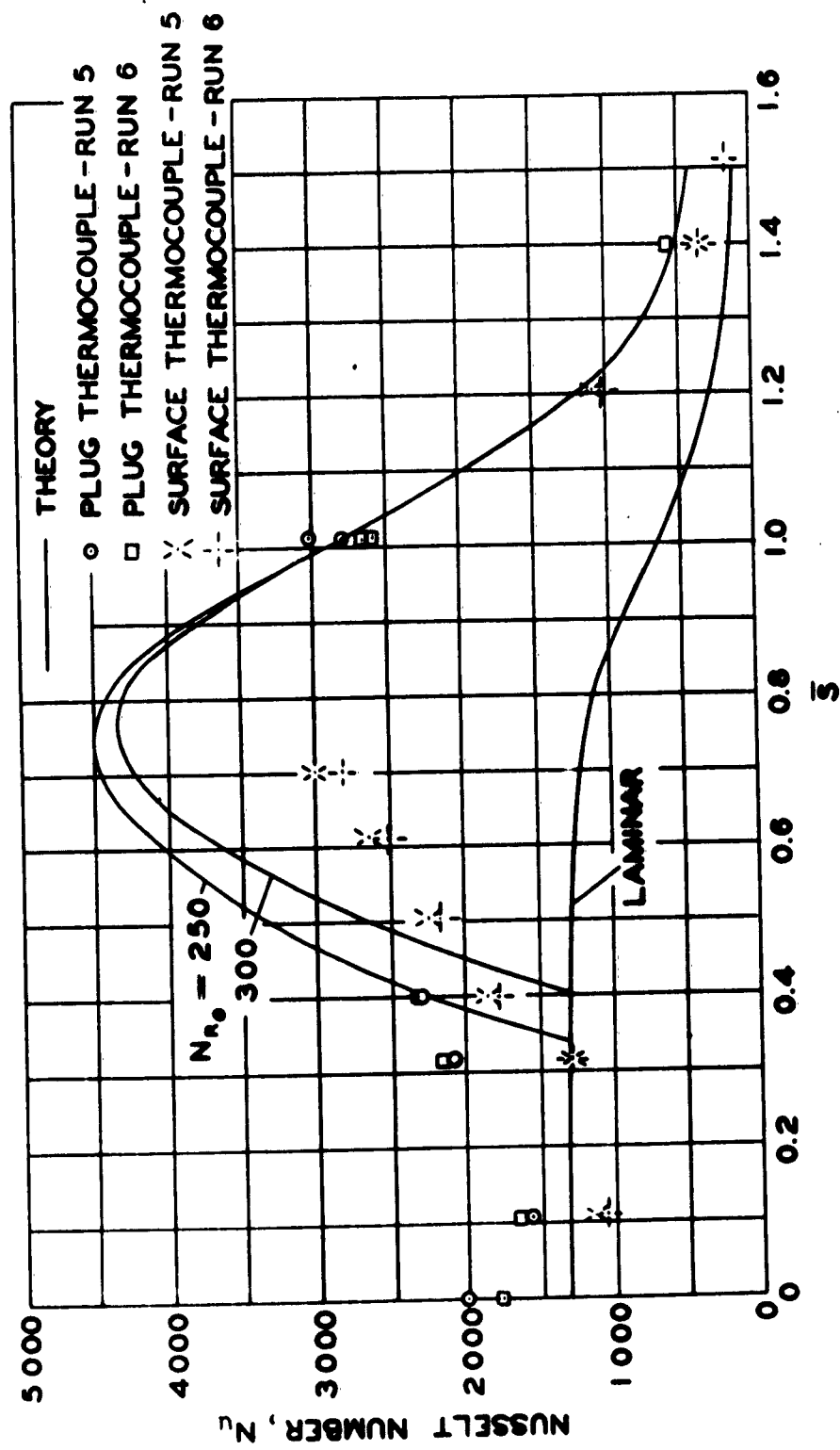


FIG. 11 VARIATION OF NUSSELT NUMBER ALONG MERIDIAN OF HEMISPHERE  
 $\bar{N}_R = 5.1 \times 10^6$  - RUN 5



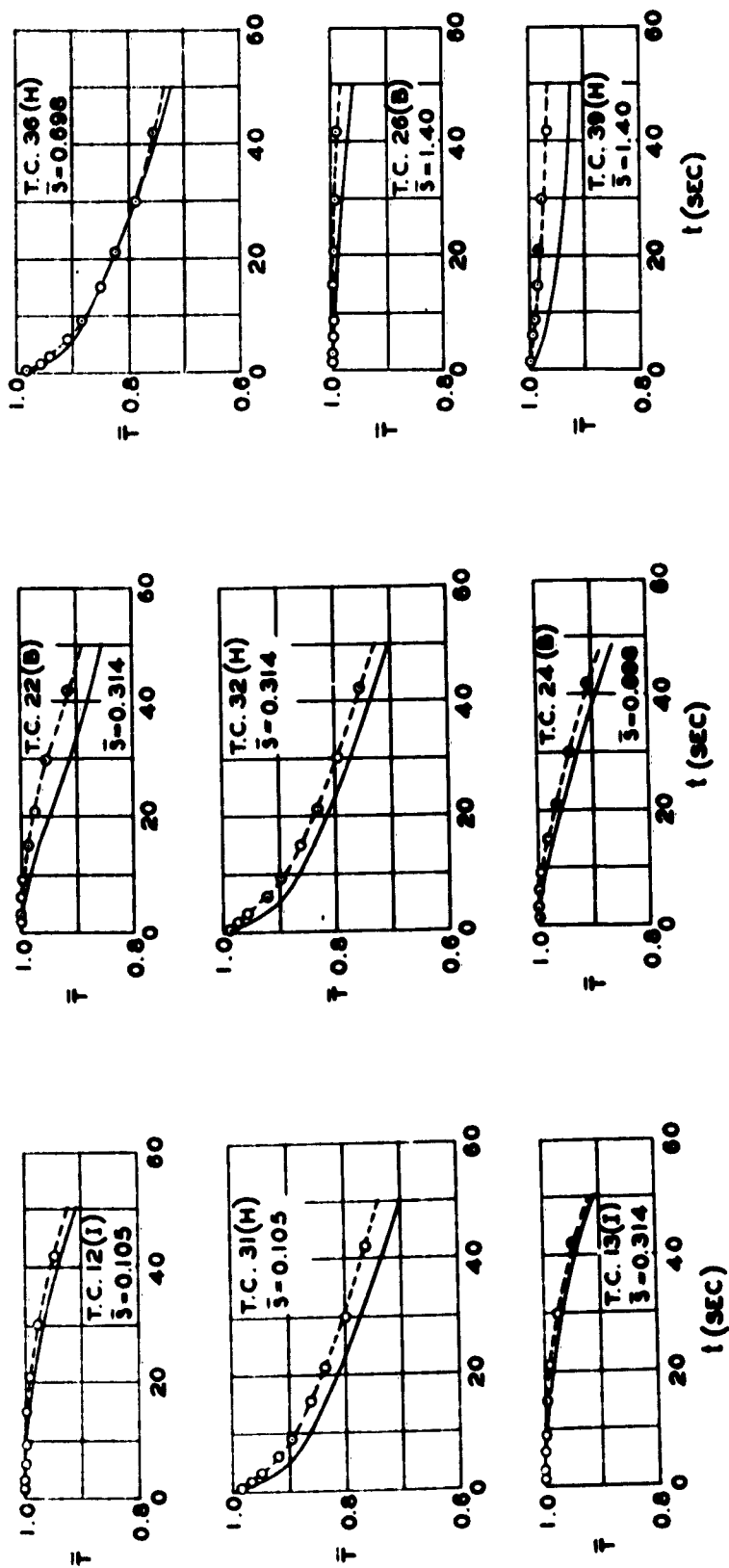


FIG. 12. COMPARISON OF EXPERIMENTAL AND CALCULATED TEMPERATURE-TIME HISTORIES RUNS 1 AND 2

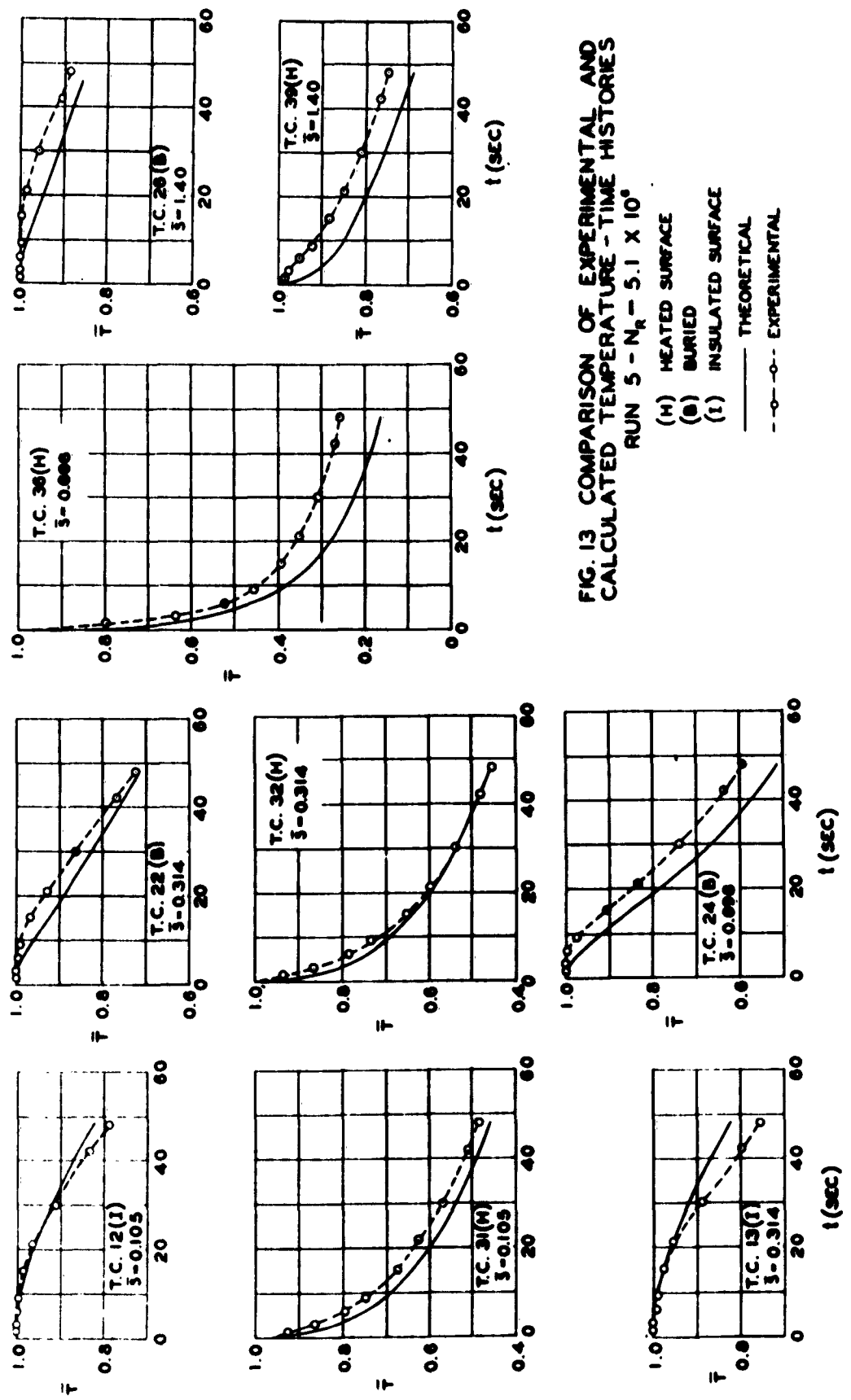


FIG. 13 COMPARISON OF EXPERIMENTAL AND  
 CALCULATED TEMPERATURE - TIME HISTORIES  
 RUN 5 -  $N_r = 5.1 \times 10^9$

**DISTRIBUTION LIST FOR UNCLASSIFIED  
TECHNICAL REPORTS ISSUED UNDER  
CONTRACT NONR 839(23), TASK NR 064-433**

Chief of Naval Research Department of the Navy Washington 25, D.C. Attn: Code 438 Code 439	(1) (1)	Director Naval Research Laboratory Washington 25, D. C. Attn: Tech. Info. Officer Code 6200 Code 6205 Code 6250 Code 6260	(6) (1) (1) (1) (1)
Commanding Officer Branch Office Office of Naval Research 495 Summer Street Boston 10, Massachusetts	(1)	Armed Services Tech. Info. Agency Arlington Hall Station Arlington 12, Virginia	(10)
Commanding Officer Office of Naval Research Branch Office John Crerar Library Building 86 E. Randolph Street Chicago 1, Illinois	(1)	Office of Technical Services Department of Commerce Washington 25, D. C.	(1)
Commanding Officer Office of Naval Research 346 Broadway New York 13, New York	(1)	Office of the Secretary of Defense Research & Development Division The Pentagon Washington 25, D. C. Attn: Technical Library	(1)
Commanding Officer Office of Naval Research Branch Office 1030 E. Green Street Pasadena, California	(1)	Chief Defense Atomic Support Agency Washington 25, D. C. Attn: Document Lib. Br.	(1)
Commanding Officer Office of Naval Research Branch Officer 1000 Geary Street San Francisco, California	(1)	Office of the Secretary of the Army The Pentagon Washington 25, D. C. Attn: ; Army Library	(1)
Commanding Officer Office of Naval Research Navy No. 100, Fleet Post Office New York, New York	(25)	Chief of Staff Department of the Army Washington 25, D. C. Attn: Develop. Br. (R & D Div.) Research Br. (R & D Div.) Spec. Weaps. Br. (R & D. .)	(1) (1) (1)

Office of the Chief of Engineers  
Department of the Army  
Washington 25, D. C.

Attns: ENG-EB Prot. Const. Br.,  
Eng. Div. Mil. Const. (1)  
ENG-HL Lib. Br. Adm. Ser.  
Div. (1)  
ENG-EA Struc. Br., Eng.  
Div. Mil. Const. (1)  
ENG-NB Special Eng. Br.  
Eng. R & D Div.) (1)  
ENG-WD Planning Div. Civ.  
Works (1)

Commanding Officer  
Engineer Research Development Lab.  
Fort Belvoir, Virginia (1)

Office of the Chief of Ordnance  
Department of the Army  
Washington 25, D. C.

Attns: Research & Materials Br.  
(Ord. R & D Div.) (1)

Commanding Officer  
Watertown Arsenal  
Watertown, Massachusetts  
Attns: Laboratory Division (1)

Commanding Officer  
Frankford Arsenal  
Bridesburg Station  
Philadelphia 37, Pennsylvania  
Attns: Laboratory Division (1)

Office of Ordnance Research  
2127 Myrtle Drive  
Duke Station  
Durham, North Carolina  
Attns: Div. of Eng. Sciences (1)

Commanding Officer  
U.S. Army Signal Res. & Dev. Lab.  
SIGFM/EL-G  
Fort Monmouth, New Jersey (1)

Chief of Naval Operations  
Department of the Navy  
Washington 25, D. C.

Attns: Op 37 (1)

Commandant Marine Corps  
Headquarters, U.S. Marine Corps  
Washington 25, D. C. (1)

Chief, Bureau of Ships  
Department of the Navy  
Washington 25, D. C.

Attns: Code 312 (2)  
Code 376 (1)  
Code 377 (1)  
Code 420 (1)  
Code 423 (2)  
Code 442 (2)

Chief, Bureau of Aeronautics  
Department of the Navy  
Washington 25, D. C.

Attns: AE-4 (1)  
AV-34 (1)  
AD (1)  
AD-2 (1)  
RS-7 (1)  
RS-8 (1)  
SI (1)  
TS-42 (1)

Chief, Bureau of Ordnance  
Department of the Navy  
Washington 25, D.C.

Attns: Ad 3 (1)  
Re (1)  
Res (1)  
Reu (1)  
ReS5 (1)  
ReS1 (1)  
Ren (1)

Special Projects Office  
Bureau of Ordnance  
Department of the Navy  
Washington 25, D.C.  
Attns: Missile Branch (2)

Chief, Bureau of Yards & Docks  
Department of the Navy  
Washington 25, D.C.

Attn: Code D-202 (1)  
Code D-202.3 (1)  
Code D-220 (1)  
Code D-222 (1)  
Code D-410C (1)  
Code D-440 (1)  
Code D-500 (1)

Commanding Officer & Director  
David Taylor Model Basin  
Washington 7, D. C.

Attn: Code 140 (1)  
Code 600 (1)  
Code 700 (1)  
Code 720 (1)  
Code 725 (1)  
Code 731 (1)  
Code 740 (2)

Commander  
U.S. Naval Ordnance Laboratory  
White Oak, Maryland  
Attn: Technical Library (2)  
Technical Evaluation Dep.(1)

Director  
Materials Laboratory  
New York Naval Shipyard  
Brooklyn 1, New York (1)

Commanding Officer & Director  
U.S. Naval Electronics Lab.  
San Diego 52, California (1)

Officer-in-Charge  
Naval Civil Engineering Research  
and Evaluation Laboratory  
U.S. Naval Construction  
Battalion Center  
Port Hueneme, California (2)

Director  
Naval Air Experimental Station  
Naval Air Material Center  
Naval Base  
Philadelphia 12, Pennsylvania  
Attn: Materials Laboratory (1)  
Structures Laboratory (1)

Officer-in-Charge  
Underwater Explosion Research Div.  
Norfolk Naval Shipyard  
Portsmouth, Virginia  
Attn: Dr. A.H. Keil (2)

Commander  
U.S. Naval Proving Grounds  
Dahlgren, Virginia (1)

Commander  
Naval Ordnance Test Station  
Inyokern, China Lake, California  
Attn: Physics Division (1)  
Mechanics Branch (1)

Commander  
Naval Ordnance Test Station  
Underwater Ordnance Division  
3202 E. Foothill Boulevard  
Pasadena 8, California  
Attn: Structures Division (1)

Commanding Officer & Director  
Naval Engineering Experiment Station  
Annapolis, Maryland

Superintendent  
Naval Post Graduate School  
Monterey, California (1)

Commandant  
Marine Corps Schools  
Quantico, Virginia  
Attn: Director, Marine Corps  
Development Division (1)

Commanding General  
U.S. Air Force  
Washington 25, D.C.  
Attn: Research & Devel. Div. (1)

Commander  
Air Material Command  
Wright-Patterson Air Force Base  
Dayton, Ohio  
Attn: MCREX-B (1)  
Structures Division (1)

Commander  
U.S. Air Force Institute of Tech.  
Wright-Patterson Air Force Base  
Dayton, Ohio=  
Attn: Chief, Applied Mechanics  
Group (1)

Director of Intelligence  
Headquarters, U.S. Air Force  
Washington 25, D.C.  
Attn: P.V. Branch  
(Air Targets Division)(1)

Commander  
Air Force Office of Scientific Res.  
Washington 25, D.C.  
Attn: Mechanics Division (1)

U.S. Atomic Energy Commission  
Washington 25, D.C.  
Attn: Director of Research (2)

Director  
National Bureau of Standards  
Washington 25, D.C.  
Attn: Division of Mechanics (1)  
Engineering Mecha. Sect.(1)  
Aircraft Structures (1)

Commandant  
U.S. Coast Guard  
1300 E Street, N.W.  
Washington 25, D.C.  
Attn: Chief, Testing & Devel.  
Division (1)

U.S. Maritime Administration  
General Admin. Office Building  
Washington 25, D.C.  
Attn: Chief, Div. of Preliminary  
Design (1)

National Aeronautics & Space  
Administration  
1512 H Street, N.W.  
Washington 25, D.C.  
Attn: Loads & Structures Div. (2)

Director  
Langley Aeronautical Laboratory  
Langley Field, Virginia  
Attn: Structures (2)

Director  
Forest Products Laboratory  
Madison, Wisconsin (1)

Civil Aeronautics Administration  
Department of Commerce  
Washington 25, D.C.  
Attn: Chief, Aircraft Engineering  
Div. (1)  
Chief, Airframe & Equipment  
D (1)

Professor Lynn S. Beedle  
Fritz Engineering Laboratory  
Lehigh University  
Bethlehem, Pennsylvania (1)

Professor R. L. Bisplinghoff  
Dept. of Aeronautical Engineering  
Massachusetts Inst. of Technology  
Cambridge 39, Massachusetts (1)

Professor H. H. Bleich  
Department of Civil Engineering  
Columbia University  
New York 27, New York

Professor B. A. Boley  
Department of Civil Engineering  
Columbia University  
New York 27, New York

National Sciences Foundation  
1520 H Street, N.W.  
Washington, D.C.  
Attn: Engineering Sciences Division(1)

Professor G. F. Carrier  
Pierce Hall  
Harvard University  
Cambridge 38, Massachusetts

National Academy of Sciences 2101 Constitution Avenue Washington 25, D.C. Attn: Tech. Director, Comm. on Ships' Structural Design Exec. Sec'ty, Comm. on Under- sea Warfare	(1)	Professor N.J. Hoff, Head Division of Aeronautical Engrg. Stanford University Stanford, California	(1)
Professor Herbert Deresciewicz Dept. of Civil Engineering Columbia University 632 W. 125th Street New York 27, New York	(1)	Professor W.H. Hoppmann, II Dept. of Mechanics Rensselaer Polytechnic Inst. Troy, New York	(1)
Professor D.C. Drucker, Chairman Division of Engineering Brown University Providence, Rhode Island	(1)	Professor Bruce G. Johnston University of Michigan Ann Arbor, Michigan	(1)
Professor A.C. Eringen Dept. of Aeronautical Engineering Purdue University Lafayette, Indiana	(1)	Professor J. Kempner Dept. of Aerospace Engrg. and Applied Mechanics Polytechnic Institute of B'klyn. 333 Jay Street Brooklyn 1, New York	(1)
Professor W. Flugge Dept. of Mechanical Engineering Stanford University Stanford, California	(1)	Professor H.L. Langhaar Dept. of Theoretical and Appl. Mech. University of Illinois Urbana, Illinois	(1)
Professor J. N. Goodier Dept. of Mechanical Engineering Stanford University Stanford, California	(1)	Professor B.J. Lazan, Director Engineering Experiment Station University of Minnesota Minneapolis 14, Minnesota	(1)
Professor L.E. Goodman Engineering Experiment Station University of Minnesota Minneapolis, Minnesota	(1)	Professor E.H. Lee Division of Applied Mathematics Brown University Providence 12, Rhode Island	(1)
Professor M. Hetenyi The Technological Institute Northwestern University Evanston, Illinois	(1)	Professor George H. Lee Director of Research Rensselaer Polytechnic Institute Troy, New York	(1)
Professor P.G. Hodge, Jr. Dept. of Mechanics Technology Center Illinois Inst. of Technology Chicago 16, Illinois	(1)	Mr. M.M. Lemcoe Southwest Research Institute 8500 Culebra Road San Antonio 6, Texas	(1)
		Professor Paul Lieber Geology Department University of California Berkeley 4, California	(1)

Professor R.D. Mindlin  
Dept. of Civil Engineering  
Columbia University  
632 W. 125th Street  
New York 27, New York

(1)

Professor Paul M. Naghdi  
Building T-7  
College of Engineering  
University of California  
Berkeley 4, California

(1)

Professor William A. Nash  
Dept. of Engineering Mechanics  
University of Florida  
Gainesville, Florida

(1)

Professor N.M. Newmark, Head  
Dept. of Civil Engineering  
University of Illinois  
Urbana, Illinois

(1)

Professor Aris Phillips  
Dept. of Civil Engineering  
15 Prospect Street  
Yale University  
New Haven, Connecticut

(1)

Professor W. Prager, Chairman  
Physical Sciences Council  
Brown University  
Providence 12, Rhode Island

(1)

Professor E. Reissner  
Dept. of Mathematics  
Massachusetts Inst. of Technology  
Cambridge 39, Massachusetts

(1)

Professor M.A. Sadowsky  
Dept. of Mechanics  
Rensselaer Polytechnic Institute  
Troy, New York

(1)

Professor J. Stallmeyer  
Dept of Civil Engineering  
University of Illinois  
Urbana, Illinois

(1)

Professor Eli Sternberg  
Dept. of Mechanics  
Brown University  
Providence 12, Rhode Island

(1)

Professor S.P. Timoshenko  
School of Engineering  
Stanford University  
Stanford, California

(1)

Professor A.S. Velesztos  
Dept. of Civil Engineering  
University of Illinois  
Urbana, Illinois

(1)

Professor Dana Young  
Yale University  
New Haven, Connecticut

(1)

Dr. John F. Brahtz  
Dept. of Engineering  
University of California  
Los Angeles, California

(1)

Mr. Martin Goland, Vice President  
Southwest Research Institute  
8500 Culebra Road  
San Antonio, Texas

(1)

Mr. S. Levy  
General Electric Research Lab.  
6901 Elmwood Avenue  
Philadelphia 42, Pa.

(1)

Professor B. Budiansky  
Dept. of Mechanical Engineering  
School of Applied Sciences  
Harvard University  
Cambridge 38, Massachusetts

(1)

Professor H. Kolsky  
Division of Engineering  
Brown University  
Providence 12, Rhode Island

(1)

Professor E. Orowan  
Department of Mechanical Engrg.  
Mass. Institute of Technology  
Cambridge 39, Massachusetts

(1)

Professor J. Ericksen  
Mechanical Engrg. Department  
John Hopkins University  
Baltimore 18, Maryland

(1)

Professor T.Y. Thomas  
Graduate Institute for Mathematics  
and Mechanics  
Indiana University  
Bloomington, Indiana

(1)



Professor Joseph Martin, Head Dept. of Engineering Mechanics College of Engrg. and Architecture Pennsylvania State University University Park, Pennsylvania	(1)	Professor W.J. Hall Dept. of Civil Engineering University of Illinois Urbana, Illinois	(1)
Mr. K.H. Koopman, Secretary Welding Research Council of The Engineering Foundation 29 West 39th Street New York 18, New York	(2)	Project Staff	(10)
		For your future distribution	(10)
Professor Walter T. Daniels School of Engrg. and Architecture Howard University Washington 1, D.C.	(1)		
Dr. D.O. Brush Structures Department 53-13 Lockheed Aircraft Corporation Missile Systems Division Synnyvale, California	(1)		
Professor Nicholas Perrone Engineering Science Dept. Pratt Institute Brooklyn 5, New York	(1)		
Legislative Reference Service Library of Congress Washington 25, D.C. Attn: Dr. E. Wenk	(1)		
Commander Wright Air Development Center Wright-Patterson Air Force Base Dayton, Ohio Attn: Dynamics Branch	(1)		
	(1)		
	(1)		
	(1)		
Commanding Officer USNNOEU Kirtland Air Force Base Albuquerque, New Mexico Attn: Code 20 (Dr. J.N. Brennan)	(1)		
Professor J.E. Cermak Dept. of Civil Engineering Colorado State University Fort Collins, Colorado	(1)		